RSC Advances

ROYAL SOCIETY OF CHEMISTRY

www.rsc.org/advances

Cite this: DOI: 10.1039/c0xx00000x

www.rsc.org/xxxxxx

ARTICLE TYPE

A stable Bi_2S_3 Quantum Dot-Glass nanosystem: Size tuneable photocatalytic hydrogen production under solar light

Sunil R. Kadam, Rajendra P. Panmand, Ravindra S. Sonawane, Suresh W. Gosavi and Bharat B. Kale*

Received (in XXX, XXX) XthXXXXXXXXX 20XX, Accepted Xth XXXXXXXXX 20XX

DOI: 10.1039/b000000x

The present work comprises a novel approach to design Bismuth sulfide (Bi_2S_3) quantum dots (QD's) glass nanocomposite system by confining nano Bi_2S_3 in designated glass composition for solar light driven hydrogen (H_2) production. Numerous methods have been reported for the synthesis of Bi_2S_3, however, we have demonstrated the synthesis of Bi_2S_3 QD's (0.5-0.7%) in the silicatete glass using melt and quench method. X-Ray diffraction and electron diffraction patterns of glass nanosystem exhibits orthorhombic crystallite system of the Bi_2S_3 QD's. Transmission Electron Microscopy demonstrates that the 3-5 and 7-10 nm size Bi_2S_3 QD's distributed homogeneously in a monodispersed form in the glass domain and on the surface with a ''partially embedded exposure'' configuration. The role of glass on control of size and shape of Bi_2S_3 QD's and their effect on the photocatalytic hydrogen generation has been discussed. The utmost H_2 production *i.e.* 6418.8 µMole $h^{-1}g^{-1}$ was achieved for the Bi_2S_3 –glass nanosystem under solar light irradiation.This glass nanosystem instruct an excellent photo stability against photocorrosion and also a facile catalytic function. Therefore, even a very small amount of Bi_2S_3 QD's is able to photodecompose H_2S and produce hydrogen under visible light.The salient features of this QD's glass nanosystem are reusability after simple washing, enhanced stability and remarkable catalytic activity.

Introduction

The metal sulfide QD's semiconductor have generated a great deal of interest in a wide range of field of science and technology.[1,2] The need for search clean energy generation technology has lead to the surge in renewable energy research. Nowadays, hydrogen (H_2) generation has significance as a clean fuel.[3-5] Utilization of solar energy for the production of H_2 using visible light active semiconductor photocatalyst is attracting much attention because of global problem related to energy and environment.[6-8] Presently, hydrogen produced from water using conventional steam reforming of methane is quite expensive. Hydrogen sulfide (H_2S) is a waste released by oil and natural gas refineries (15-20%). Also, alkali industries and many agrochemical industries produce H_2S as a by product. Hence, the environment pollutant, H_2S is abundantly available and needs to use for H_2 production as clean energy fuel.[9] Hence, the production of H_2 via photocatalytic splitting of H_2S has great significance.There are reports on oxide based catalyst such as TiO_2, ZnO for good photocatalytic H_2 production.[10, 11] However, solar spectrum contains only 5% of UV light and did not show good activity in the solar light.[12-14] Researchers have also developed the visible light active catalyst such as CdS, CdSe and CdSSe.[7, 15] The CdS is reported as a best visible light active photocatalyst, however use of CdS is restricted due to the photocorrosion problem.[16, 17]It is quite well known that photocatalytic activity depend on the particle size. Lower particle size has more surface area and hence more active sites are available for photocatalytic activity.[15] However, due to the stability problem, search for new highly efficient stable visible light active photocatalyst is indispensable. To overcome this stability problem, synthesis of Bi_2S_3 QD's in glass matrix has been carried out by melt and quench method to enhance the stability of the QD's. Nanoscaling of the light absorber can be of merit in case of low conductivity.When charge carriers have short lifetimes then it offer an opportunity to fine-tune the band energies of system via quantum confinement.[8] It is well known that the effect of quantum confinement on the optical activity, which has been only recently applied for controlling charge transfer in photocatalysis.[18] Such nanosystems shows the significant enhancement in the photocatalytic solar H_2 production.

In the present investigation, we have developed the Bi_2S_3 QD's (0.5-0.7 %) – glass nanosystem and tuned the size of Bi_2S_3 QD's with striking temperature. The glass nanosystem has been characterized thoroughly for the investigation of structural and optical properties. The effect of Bi_2S_3 QD's size on the hydrogen production has been demonstrated for the first time. It is

noteworthy that the H_2 production achieved is much higher than the reported bulk Bi_2S_3 powder photocatalyst.[19]

Experimental Section

Material preparation

The all chemicals used were of A.R. grade purchased from M/s S.D. Fine Chemicals, Mumbai, India. The multi component glass composition *i.e* 52% SiO_2, 10% Na_2O, 6% MgO, 6% B_2O_3, 12% K_2O, 10% ZnO, and 4% TiO_2has been designed. The bulk Bi_2S_3 synthesized by hydrothermal method is used as a source of Bi_2S_3 QD's for nanocomposite which is introduced in the glass directly. The composition was mixed thoroughly using a pestle and mortar to obtain a homogeneous mixture. The same homogeneous mixture was melted in a recrystallized alumina crucible using an electrically heated muffle furnace (Thermolyne-U3200) at 1100-1150 °C. The glass melt was mechanically homogenized at the same temperature for 2 hr. After refining, the glass melt was air quenched on a preheated brass plate and processed immediately for annealing. The glass was annealed in a programmable furnace at its transition temperature (Tg) *i.e.* 450-500 °C and cooled down slowly to room temperature to remove the stresses. The doped glass was cut into three pieces. To study the effect of temperature and time of annealing on crystallization of Bi_2S_3 in the glass matrix, the cut pieces of as prepared glass nanosystems were heat treated at 550, 575 and 600 °C for 8 hrs. The identification of the samples is given in Table 1.

Table 1. Identification Table

Sample Code	% doping
GP - 11	0.5
GP -12	0.6
GP – 14	0.7

Material characterization

The crystalline phases and the crystallite size of the photocatalyst was investigated using X-ray powder diffraction (XRD) technique (XRD, Advance D8, Bruker-AXS). Room temperature micro Raman scattering (RS) was performed using a HR 800-Raman Spectroscopy, Horiba JobinYvon, France, with an excitation at 632.81nm by a coherent He–Ne ion laser and a liquid nitrogen cooled CCD detector. The optical properties of the powder samples were studied using an UV-Visible-Near Infrared spectrometer (UV-Vis-NIR, Perkin Elmer Lambda-950) and Photoluminescence spectrofurometer(Horiba JobinYvon Fluorolog3). The morphologies of the Bi_2S_3 QDs glass nanocomposites were investigated by High resolution transmission electron microscopy (HRTEM, JEOL, 2010F). For HRTEM studies, the samples were prepared by dispersing the glass powder in ethanol, followed by sonication in an ultrasonic bath for 5 min and then drop-casting the sample on a carbon coated copper grid and by subsequent drying in a vacuum. The Collected gas sample was analysed using a GC system (Shimadzu GC-2025) coupled with TCD detector and packed column (ShinCarbon ST).

Photocatalytic study for H_2S splitting

The photocatalytic activity was carried out in cylindrical quartz reactor filled with 700 ml 0.5 M KOH. At room temperature, the vigorously stirred suspension was purged with argon for 1 h and then hydrogen sulphide (H_2S) was bubbled through the solution for about 1 h. Each experiment was carried out in identical condition with H_2S flow 2.5 ml min^{-1}. The catalyst were introduced as a suspension into a reactor and irradiated with Xe-lamp light source (LOT ORIEL GRUPPE, EUROPA, LSH302, for Xe lamp spectrum) of intensity 300 W. The generated H_2 was collected in the graduated eudiometric tube. The purity of the collected gas was analyzed by gas chromatograph (Model Schimadzu GC-14B, MS-5 Å column, TCD, Ar carrier).

Results and Discussion

The Bi_2S_3 QD's glass nano system has been fabricated using different wt% of guest material *i.e.* Bi_2S_3 (0.5-0.7%). All the glass compositions were tested for their Bi_2S_3 dissolution ability within the matrix during the melting process, which is the key step in fabricating Bi_2S_3 QD's glass entities. The Bi_2S_3 QD's glass nanocomposite such as GP-11, GP-12 and GP-14 were synthesized by melt and quench method and analyzed by XRD (Fig. 1). The XRD pattern is having broad hump in the 2θ range of 20-40° with some weak/ noisy peaks of Bi_2S_3/Bi signifying the amorphous glass containing Bi_2S_3/Bi nanoparticles. The XRD pattern of sample GP-11 (0.5% Bi_2S_3) shows increase in peak intensity of 2θ= 28.40° (230) and 27.36° (021) indicative of the presence of orthorhombic Bi_2S_3 in glass matrix which matches well with the JCPDS Card No. 06-0333. It is observed that with increase in doping of Bi_2S_3 powder in glass matrix, the intensity of peak at 2θ= 28.40° decreases, whereas, the peak at 2θ= 27.36° slightly shifted to 27.12° which is very close to (012) plane of rhombohedral bismuth (JCPDS Card No. 85-1331).It reveals that with increase in Bi_2S_3 doping percentage in glass, there is a formation of little Bi along with Bi_2S_3. However, the XRD of sample GP-11 indicate the presence of Bi_2S_3 only. The higher concentration of Bi_2S_3 may leads into the slight decomposition of Bi_2S_3 to Bi during melting. At lower concentration of Bi_2S_3 the dissolution of Bi_2S_3 in glass matrix is adequate. However, at higher concentration of Bi_2S_3 doping, the dissolution takes longer time at melting condition which leads to decoposition of Bi_2S_3 present at the surface to Bi. Hence, lower doping shows only Bi_2S_3 and higher doping shows slight formation of Bi which is quite obvious. The presence of Bi_2S_3 in glass matrix also confermed by EDX (see supporting iformation figure S-1).

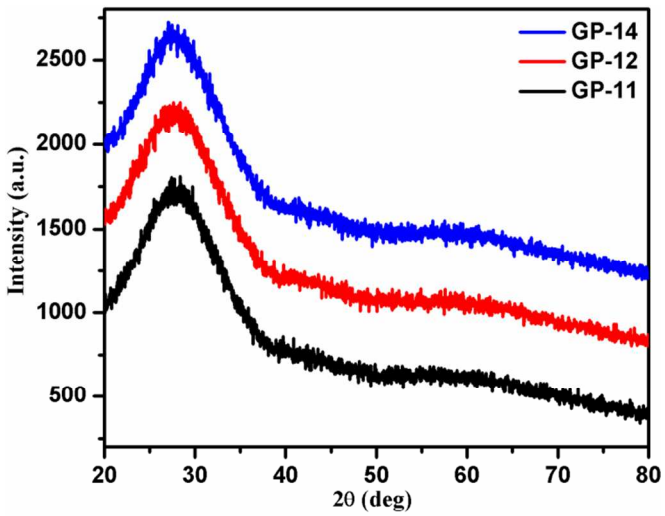

Fig. 1: XRD spectra of Bi_2S_3 Glass composite GP-11, GP-12 and GP-14.

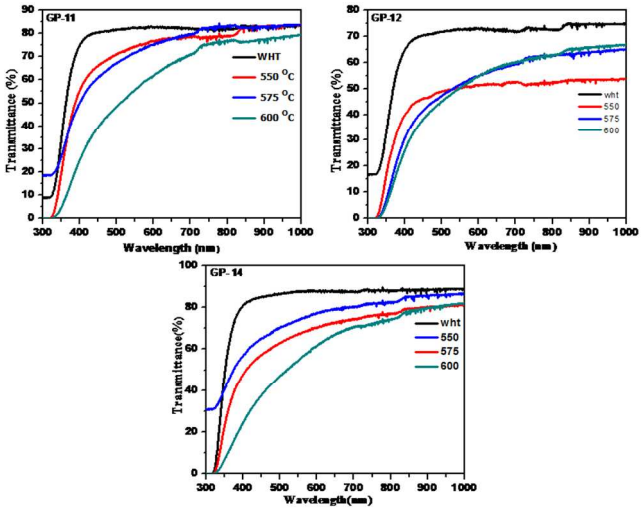

Fig. 2: Transmittance spectra of Bi_2S_3 glass GP-11, GP-12 and GP-14.

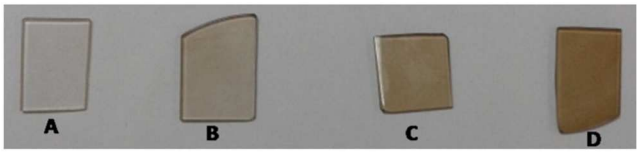

Fig. 3 Actual photograph of GP-11 (0.5 wt %). A) As prepared glass, B) heat treated glass at 550 °C for 8 hrs, C) heat treated glass at 575 °C for 8 hrs and D) heat treated glass at 600 °C for 8 hrs

The UV-Vis-NIR transmittance spectra of 0.5% to 0.7 % Bi_2S_3 doped glass nanosystemis shown in Fig. 2.The transmittance edge shows the strong red shift with increase in annealing temperature. This may be due to the growth of Bi_2S_3nanoparticles into the glass *i.e* quantum confinement effect. The average band gap of Bi_2S_3 glass nanocomposite obtained from the Tauc plot (see supporting information Fig. S-2) is in the range of 3.55 to 2.50 eV for as prepared and heat treated glass nanocomposite samples. It is concluded that the band gap of the glass nanocomposite is shifted from 3.55 to 2.50 eV with change in size of Bi_2S_3QD's. As prepared glass is of pale yellow in colour and after heat treatment it changes to dark yellow/brown depending on heat treatment temperature (see Fig 3 for actual photograph of glass nanocomposites). The colour obtained to the glass ascribed to the growth of Bi_2S_3 or Bi QD's into the glass matrix.The drastic shift in the band gap of the glass nanosystems is attributed to a strong quantum confinement effect of the Bi_2S_3 QD's. When the particle size is less than the Bohr radius, the materials are in the strong confinement region, and both electron and hole confinement were assumed to be dominant relative to the Coulomb interaction.[20, 21] This results in the splitting of both valence and conduction bands into a series of sub-bands, and a band gap is occured between the top of the sub-band of the valence band and the bottom of the sub-band of the conduction band.[22] The band gap energy due to the confinement is shown as per the equation (1).

$$E = E_g + \frac{\pi^2 \hbar^2}{2\mu R^2} \text{--------} \quad (1)$$

Where, E_g is the energy of the band gap of the semiconductor bulk crystal, μ is the electron and hole effective mass, and R is the radius of the QD's in glass matrix. The calaculated size of Bi_2S_3 particles in glass heat treated at 550 and 600 °C(for 8 hr) from the quantum confinement approximation are 4.6 and 11 nm. These sizes are slightly higher than the sizes observed from TEM analysis (3-4 and 7-10 nm). It may be due to the QD's embedded in amorphous glass matrix.

Photoluminescence spectra of as prepared and heat treated sample were shown in Fig.4.The samples were analysed using excitation wavelength 350 nm. It is observed that in all spectra, there is broad emission band centred at ~535 nm,which is quenching with increasing heat treatment temperature *i.e.* 550 °C to 600 °C. The peak appeared at 629 nm and 668 nm also decreases with increase in heat treatment. It may be due to the increase in the particle size. After increasing the particle size, the strain is developed in the glass which produces defects in the glasses. Hence, due to the more number of defects, the intensity of the peaks reduces, drastically.Growth of the QD's decreases the surface to volume ratio and thereby increases the quenching of the photoluminescence at the surface of the QDs.[18]

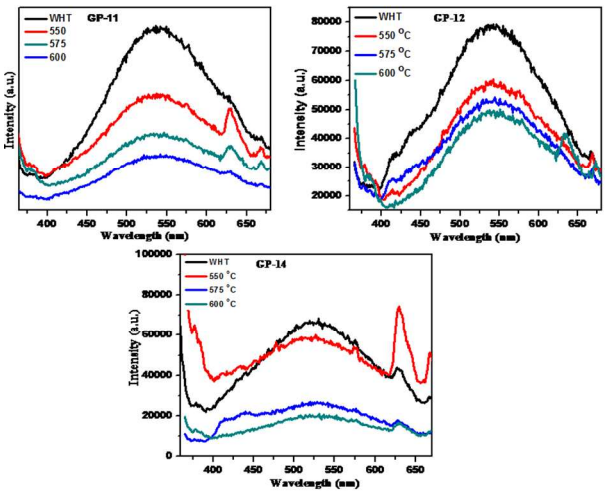

Fig. 4: PL spectra of Bi_2S_3 glass GP-11(0.5%), GP-12(0.6) and GP-14 (0.7%) as a function of striking temperature.

Raman spectroscopy is an effective method for structural characterization of the materials.[23]Room-temperature Raman spectra of Bi_2S_3 powder synthesized by hydrothermal and Bi_2S_3 QD's glass nanocomposite, were recorded in the range 50-1500 cm^{-1} and results are depicted in Fig.5 a & b, respectively. Raman study shows characteristics peak at 92.6, 115.2, 137.8, 205.8, 306 and 432 cm^{-1} for Bi_2S_3 powder synthesized by hydrothermal, which are in good agreement with values for commercial Bi_2S_3 as well as nanoparticles reported by Robin *et.al*[24] Raman spectrum of Bi_2S_3 glass composite shows characteristic peaks at ~98.5, 114, 198, 185 and 230. which are in good agreement with Bi_2S_3.[25] The Raman spectrum of Bi_2S_3 in glass show nearly similar visual appearance like Bi_2S_3 powder. The Raman spectrum of Bi_2S_3 QD's in glass presented here may be serve as a reference for future identification.The intensity of peak located at 114 cm^{-1} increase with increase in wt. % of Bi_2S_3in glass matrix. It is quite obvious because the concentration of Bi_2S_3 QD's were also increased with increase in dopant percent.

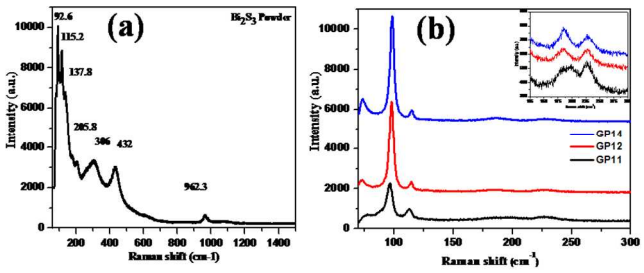

Fig.5: Raman spectra of a) Bi_2S_3 powder b) Bi_2S_3 glass GP-11, GP-12, and GP-14 heat treated at 600 °C for 8 hr

The Bi_2S_3 glass sample, after heat treatment at 550 and 600 °C (for 8 hr) was crushed into a fine powder and used for TEM analysis. From the TEM images (Fig. 6&7), it is quite clear that spherical Bi_2S_3 QD's are homogeneously distributed in the glass matrix. The size of the Bi_2S_3 QD's is observed to be 3-4 nm and 7-10 nm for samples heat treated at 550 and 600°C (for 8 hr), respectively. The Selected Area Electron Diffractionpattern (Fig. 6d) pattern shows the single crystalline nature of the Bi_2S_3 QD's.

During the glass melting, Bi_2S_3 dissociates into Bi and S ions and dispersed into the glass matrix. The heat treatment of glass at its softening temperature results in the growth of Bi_2S_3QD's via nucleation and crystal growth mechanism. The further growth of these QD's is accelerated by prolonged thermal treatment at high temperature due to Ostwald ripening.[1,26,27] Possible growth mechanism is schematically shown in Fig. 8.

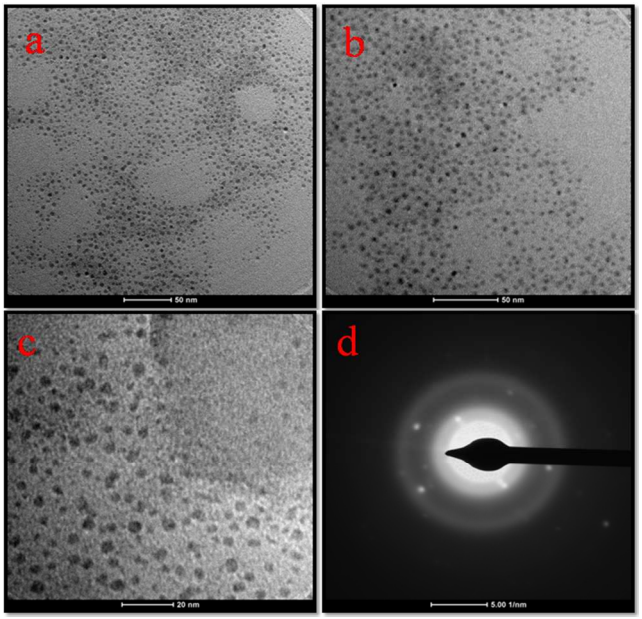

Fig.6: TEM images (a-d) for the Bi_2S_3 glass GP-14 550°C for 8 hr.

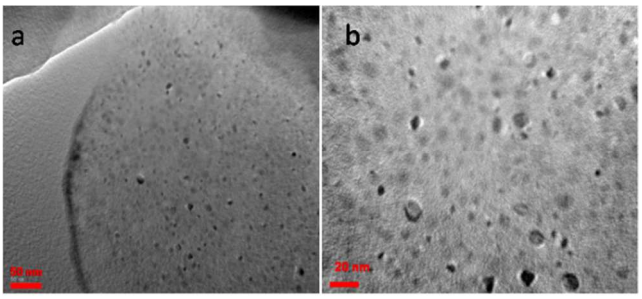

Fig.7: TEM images (a, b) for the Bi_2S_3 glass GP-14 600°C for 8 hr.

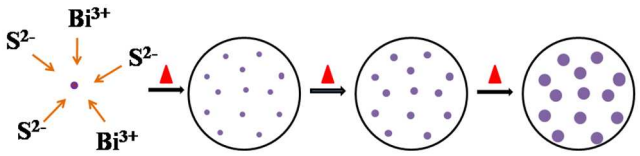

Fig.8: Schematic illustradtion of formation and growth mechanism of Bi_2S_3 QD's in glass matrix.

Photocatalytic Hydrogen Evolution

Considering the band gap of synthesized Bi_2S_3 QD's glass composite material, the photocatalytic activity for hydrogen evolution from H_2S was carried out in presence of visible light.The hydrogen generation data is summarized in Table 2 and time dependent hydrogen in Fig. 9.

Table 2 Photocatalytic H_2 evolution using glass nanosystem .

Sample Code	% doping	550ºC	575ºC	600ºC
GP 11	0.5	5544	5312.4	5122.8
GP 12	0.6	5970	5580	5296
GP 14	0.7	6418.8	6138	5636

The maximum H_2 generation *i.e* 6418.8 µmole $h^{-1}g^{-1}$ was achieved for the GP-14 striked glass at 550 °C.It is observed that with increase in particle size of Bi_2S_3 QD's, photocatalytic activity goes on decreasing which is quite obvious. The obtained results are much higher than the previously reported bulk Bi_2S_3 semiconductor catalyst.[19] For comparative study, the H_2 generation activity of bulk Bi_2S_3 sample were studied at identical conditions, which observed to be lower than the Bi_2S_3 QD's in glass matrix (see supporting information Table S-1). The higher H_2 generation obtained in the present case can be ascribed to the lower size of Bi_2S_3 QD's (3-4 nm). Due to the slightly higher striking temperature the crystal growth was slightly more, resulting in the larger QD's (7-10nm) in the silicate glass matrix. This also creates the structural defects in the glass (as discussed in photoluminescence study) which enhances the electron hole recombination.[18,28] Hence, decrease in H_2 generation with striking temperature has been observed.

Fig. 9 shows the comparative time dependent H_2 generation study with varying the doping of Bi_2S_3 concentration in the glass matrix. At higher dopant concentrations, the density of QD's is also increased in glass matrix which ultimately enhance H_2 generation. The linearity of the graph clearly depicts the stable H_2 generation.

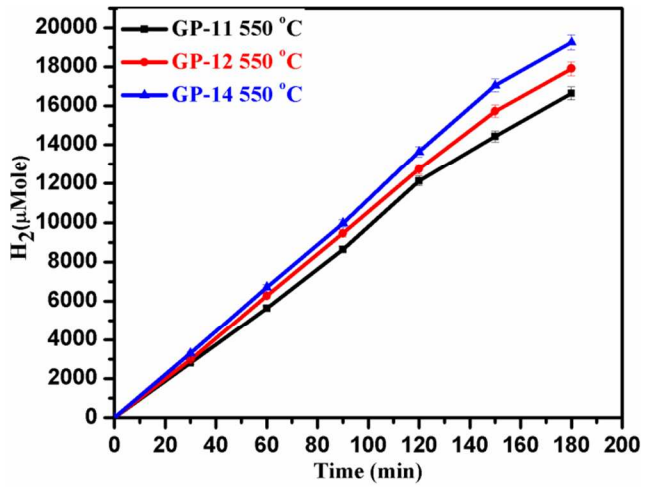

Fig.9. Photocatalytic activity obtained for glass GP-11, GP-12 and GP-14 heat treated at 550 ºC for 8 hr.

The photocatalytic H_2 generation via H_2S splitting catalysed by Bi_2S_3 QD's Semiconductor is as follows:

$$H_2S + HO^- \longleftrightarrow HS^- + H_2O$$

$$Bi_2S_3 \text{ QD's Semiconductor} \xrightarrow{h\nu} h^+_{VB} + e^-_{CB}$$

$$\text{Oxidation reaction: } 2HS^- + 2h^+_{VB} \longrightarrow S_2^{2-} + 2H^+$$

$$\text{Reduction reaction: } 2H^+ + 2e^-_{CB} \longrightarrow H_2$$

In 0.5 M KOH solution having pH 12.5 (pKa= 7.0), the weak diprotic acid H_2S (pKa= 11.96) dissociates and maintain **an** equilibrium with HS^- ions. The Bi_2S_3/Bi QD's absorb the visible light and generate the electron (e^-) and hole (h^+). Due to the small size and more surface area, generated (e^-) and (h^+) easily transport to the surface of the catalyst and readily available for the photocatalytic activity. The photogenerated h^+ from catalyst in valence band oxidizes the HS^- ion to proton (H^+) and disulfide (S_2^{2-}) ion. The photogenerated e^- in conduction band from the catalyst generates the molecular H_2 by reducing the proton.

The beauty of catalyst is that it can be reused several times for photocatalytic activity without retaining its activity. The XRD of recycled sample shown in supporting information (fig.S-3) which clearly shows the stability of the catalyst. The hydrogen evolution for recycled catalyst is quite stable(Fig.S4 and Table S2). Due to higher density of the catalyst, it settled down very fast, therefore almost complete amount of catalyst can be recovered without loss during recovery. Hence, Bi_2S_3 QD's glass nanocomposite has more significance than bulk Bi_2S_3 semiconductor powder catalyst.From the study, it is observed that higher H_2 evolution is obtained for the glass nanocomposite having lower QD's size. It is note worthy that H_2 evolution can be enhanced further with increase in density of lower size Bi_2S_3 QD's in the glass. Hence, fabrication of such nano system is in progress with tunning of glass composition.

Conclusion:

The Bi_2S_3 QD's glass nanocomposites have been successfully developed using melt and quench method. The Bi_2S_3 QD's size can be tuned 3-4 and 7-10 nm with controlled heat treatment at 550 and 600 °C, respectively. The bandgap of glass nanocomposite can be tuned from 3.5 to 2.5 eVwith size of Bi_2S_3 QD'S. The photocatalytic H_2 generation under solar light has been performed and utmost H_2 generation *i.e.* 6418.8 µmole $h^{-1}g^{-1}$ has been achieved, which is higher than Bi_2S_3 powder. It is noteworthy that the glass nanocomposite contain only 7 mg of Bi_2S_3 QD's. The higher H_2 evolution rate was obtained for glass nanocomposite having lower Bi_2S_3 QD's The recycle study shows the stability of photocatalyst and its facile regeration.

Acknowledgement:

The author authors would like to acknowledge the Department of Science Technology (DST, Govt. of India) and Department of Information and Electronics Technology (DietY), Ministry of Communication & IT, Gov. of India for finanacial support. We are also thankful to Executive Director, C-MET, Pune for facilities and support.

Notes and references

Centre for Materials for Electronics Technology,
Department of Electronics and Information Technology (DeitY),
Govt. of India, Panchawati, Off Pashan Road,
Pune-411008, India.bbkale@cmet.gov.in/ bbkale1@gmail.com

† Electronic Supplementary Information (ESI) available: [details of any supplementary information available should be included here]. See DOI: 10.1039/b000000x/

1. R. P. Panmand, G. Kumar, S. M. Mahajan, M. V. Kulkarni, B. B. Kale and S. W. Gosavi, *J. Mater. Chem. C*, 2013, **1**, 1203-1210.

2. N. Zhang, J. Qiu, G. Dong, Z. Yang, Q. Zhang and M. Peng, *J. Mater. Chem.*, 2012, **22**, 3154-3159.
3. J.O'M. Bockris, *Int. J. Hydrogen Energy*, 2002, **27**, 731.
4. J. A. Turner, *Science*, 2004, **305**, 972.
5. W. Lubitz and B. Tumas, *Chem. Rev.*, 2007, **107**, 3900.
6. N. S. Chaudhari, S. S. Warule, S. A. Dhanmane, M. V. Kulkarni, M. Valant and B. B. Kale, *Nanoscale*, 2013, **5**, 9383-9390.
7. S. K. Apte, S. N. Garaje, M. Valant and B. B. Kale, *Green Chem.*, 2012, **14**, 1455-1465.
8. B. B. Kale, J. O. Baeg, S. K. Apte, R. S. Sonawane, S. D. Naik and K. R. Patil, *J. Mater. Chem.*, 2007, **17**, 4297-4303.
9. I. A. Gargurevich, *Ind. Eng. Chem. Res.*, 2005, **44**, 7706.
10. N. Jiawei, S. Xu, X. Zhang, H. Y. Yang and D. D. Sun, *Adv. Funct. Mater.*, 2010, **20**, 4287-4294.
11. X. Zhang, Y. Liu, S.-T. Lee, S. Yang and Z. Kang, *Energy Environ. Sci.*, 2014, **7**, 1409-1419.
12. M. P. Elsner, M. Menge, C. Muller and D. W. Agar, *Catal. Today*, 2003, **79**, 487.
13. H. Lu, J. Zhao, L. Li, L. Gong, J. Zhang, L. Zhang, Z. Wang, J. Zhang and Z. Zhu, *Energy Environ. Sci.*, 2011, **4**, 3384.
14. S. R. Kadam, v. R. Mate, R. P. Panmand, L. K. Nikam, M. V. Kulkarni, R. S. Sonawane and B. B. Kale, *RSC Adv.*, 2014, **4**, 60626-60635.
15. S. K. Apte, S. N. Garaje, S. D. Naik, R. P. Waichal, J. Baeg and B. B. Kale, *Nanoscale*, 2014, **6,** 908-915.
16. Q. Li, B. Guo, J. Yu, J. Ran, B. Zhang, H. Yan and J. R. Gong., *J. Am. Chem. Soc.*, 2011, **133**, 10878-10884.
17. G. Ma, H. Yan, J. Shi, X. Zong, Z. Lei and C. Li., *Journal of Catalysis*, 2008, **260**, 134-140.
18. R. P. Panmand, G. Kumar, S. M. Mahajan, N. Shroff, B. B. Kale and S. W. Gosavi, *Phys. Chem. Chem. Phys.*, 2012, **14**, 16236-16242.
19. U. V. Kawade, R. P. Panmand, Y. A. Sethi, M. V. Kulkarni, S. K. Apte, S. D. Naik and B. B. Kale, *RSC Adv.*, 2014, **4**, 49295-49302.
20. Y. M. Azhniuk, A. V. Gomonnai, Y. I. Hutych, V. V. Lopushansky, I. I. Turok, V. O. Yukhymchuk and D. R. T. Zahn, *J.Appl. Phys.*, 2010, **107**, 113528.
21. H. Liu, Q. Liu and X. Zhao, *Mater. Charact.*, 2007, **58**, 96.
22. Y. M. Azhniuk, A. V. Gomonnai, Y. I. Hutych, V. V. Lopushansky, I. I. Turok, V. O. Yukhymchuk and D. R. T. Zahn, *Journal of Crystal Growth*, 2010, **312**, 1709.
23. M. Thripuranthaka, R. V. Kashid, C. S. Rout and D. J. Late., *Appl. Phys. Lett.*, 2014, **104**, 081911.
24. O. Rabin, J. M. Perez, J. Grimm, G. Wojtikewicz and R. Weissleder, *Nat. Mater*, 2006, **6**, 118-122.
25. k. trentelman, *J. Raman Spectrosc.*, 2009, **40**, 585-589.
26. S. Wageh, A. M. El-Nahas, A. A. Higazy and M. A. M. Mahmoud, *Journal of Alloys and Compounds*, 2013, **555**, 161-168.
27. M. H. Yukselici, *J. Phys.: Condens. Matter*, 2001, **13**, 6123-6131.
28. M. Kizilyalli, M. Bilgin and A. Usanmaz, 1989, **80**, 75-79.